Low-cost rapid miniature optical pressure sensors for blast wave measurements

Nan Wu,[1] Wenhui Wang,[1] Ye Tian,[1] Xiaotian Zou,[1] Michael Maffeo,[2] Christopher Niezrecki,[3] Julie Chen,[3] and Xingwei Wang[1,*]

[1]*Department of Electrical and Computer Engineering, University of Massachusetts Lowell, 1 University Avenue, Lowell, Massachusetts 01854, USA*
[2]*US Army Natick Soldier Research, Development, & Engineering Center, Natick, Massachusetts, USA*
[3]*Department of Mechanical Engineering, University of Massachusetts Lowell, 1 University Avenue, Lowell, Massachusetts 01854, USA*
**xingwei_wang@uml.edu*

Abstract: This paper presents an optical pressure sensor based on a Fabry-Perot (FP) interferometer formed by a 45° angle polished single mode fiber and an external silicon nitride diaphragm. The sensor is comprised of two V-shape grooves with different widths on a silicon chip, a silicon nitride diaphragm released on the surface of the wider V-groove, and a 45° angle polished single mode fiber. The sensor is especially suitable for blast wave measurements: its compact structure ensures a high spatial resolution; its thin diaphragm based design and the optical demodulation scheme allow a fast response to the rapid changing signals experienced during blast events. The sensor shows linearity with the correlation coefficient of 0.9999 as well as a hysteresis of less than 0.3%. The shock tube test demonstrated that the sensor has a rise time of less than 2 μs from 0 kPa to 140 kPa.

OCIS codes: (060.2370) Fiber optics sensors; (120.2230) Fabry-Perot; (230.4685) Optical microelectromechanical devices.

References and links

1. S. Okie, "Traumatic brain injury in the war zone," N. Engl. J. Med. **352**(20), 2043–2047 (2005).
2. R. G. DePalma, D. G. Burris, H. R. Champion, and M. J. Hodgson, "Blast injuries," N. Engl. J. Med. **352**(13), 1335–1342 (2005).
3. R. J. Irwin, M. R. Lerner, J. F. Bealer, P. C. Mantor, D. J. Brackett, and D. W. Tuggle, "Shock after blast wave injury is caused by a vagally mediated reflex," J. Trauma **47**(1), 105–110 (1999).
4. K. H. Taber, D. L. Warden, and R. A. Hurley, "Blast-related traumatic brain injury: what is known?" J. Neuropsychiatry Clin. Neurosci. **18**(2), 141–145 (2006).
5. S. Watson, W. N. MacPherson, J. S. Barton, J. D. C. Jones, A. Tyas, A. V. Pichugin, A. Hindle, W. Parkes, C. Dunare, and T. Stevenson, "Investigation of shock waves in explosive blasts using fibre optic pressure sensors," Meas. Sci. Technol. **17**(6), 1337–1342 (2006).
6. O. Tohyama, M. Kohashi, M. Fukui, and H. Itoh, "A fiber-optic pressure microsensor for biomedical applications," in *Solid State Sensors and Actuators, 1997. TRANSDUCERS '97 Chicago., 1997 International Conference on*, 1997), 1489–1492 vol.1482.
7. X. Juncheng, G. Pickrell, W. Xingwei, P. Wei, K. Cooper, and W. Anbo, "A novel temperature-insensitive optical fiber pressure sensor for harsh environments," Photon. Technol. Lett. **17**(4), 870–872 (2005).
8. W. Wang, N. Wu, Y. Tian, X. Wang, C. Niezrecki, and J. Chen, "Optical pressure/acoustic sensor with precise Fabry–Perot cavity length control using angle polished fiber," Opt. Express **17**(19), 16613–16618 (2009).
9. W. Wang, N. Wu, Y. Tian, C. Niezrecki, and X. Wang, "Miniature all-silica optical fiber pressure sensor with an ultrathin uniform diaphragm," Opt. Express **18**(9), 9006–9014 (2010).
10. W. N. MacPherson, M. J. Gander, J. S. Barton, J. D. C. Jones, C. L. Owen, A. J. Watson, and R. M. Allen, "Blast-pressure measurement with a high-bandwidth fibre optic pressure sensor," Meas. Sci. Technol. **11**(2), 95–102 (2000).
11. W. Parkes, V. Djakov, J. S. Barton, S. Watson, W. N. MacPherson, J. T. M. Stevenson, and C. C. Dunare, "Design and fabrication of dielectric diaphragm pressure sensors for applications to shock wave measurement in air," J. Micromech. Microeng. **17**(7), 1334–1342 (2007).
12. M. Chavko, W. A. Koller, W. K. Prusaczyk, and R. M. McCarron, "Measurement of blast wave by a miniature fiber optic pressure transducer in the rat brain," J. Neurosci. Methods **159**(2), 277–281 (2007).

#144481 - $15.00 USD Received 22 Mar 2011; revised 25 Apr 2011; accepted 13 May 2011; published 18 May 2011

1. Introduction

Exposure to a shock wave generated by a blast event can cause traumatic brain injury (TBI) [1,2]. A significant effort has been made in prior studies to better understand the propagation of blasts and their effect on TBI [3,4]. In order to model the behavior of a blast wave impacting on the brain tissues after propagating through the helmet and the skull, accurate pressure profiles need to be measured at different locations. An ideal pressure sensor used in such applications should have the following features: 1) a fast response time and large dynamic range to rapidly record changing pressure; 2) a small, unobtrusive size to allow for high spatial resolution measurement without disturbing the flow or the mechanics of the attached structure; and 3) a robust packaging to withstand the detrimental effects of the blast wave [5]. Conventional piezo-electrical pressure transducers are typically used, however these cannot satisfy all the above requirements. They are typically on the order of centimeter size, are spatially and mechanically obtrusive, and can be affected by high accelerations [5]. On the other hand, a fiber optic pressure sensor is a possible substitute for piezo-electrical transducers used to measure shock waves due to its ultra-fast dynamic response, compact size, simple structure and immunity to electro-magnetic interference (EMI).

In general, fiber optic pressure sensors reported in the literatures are based on the Fabry-Perot (FP) interferometer principle [6–9]. The FP cavity is formed by an optical fiber and a flexible diaphragm bonded on a supporting structure. Such a structure has potential to become an ideal sensor structure to measure pressure changes. The compact size of the sensor greatly enhances the spatial resolution. By changing the material and the thickness of the diaphragm, the resonant frequency of the diaphragm can be tailored. The low mass of the diaphragm and fiber reduces the sensor's mass loading and does not affect the inertial response of the substructure to which the sensor is attached.

MacPherson et al. fabricated their fiber optic sensor and tested it in a blast event [10]. The FP cavity was formed by the tip of an optical fiber and a copper diaphragm bonded at the end of a ferrule. The sensor showed a sinusoidal response to the pressure change and the linear region was from 160 kPa to 220 kPa. They tested their sensor in a blast event and compared the signals with other sensors. During the blast event test, the sensor showed a rise time of 3 μs with a dynamic range of 100 kPa. In another paper published in 2006 from the same group [5], a 1 μm thickness silicon dioxide diaphragm was used to bond on a pre-etched silicon supporting structure to form an FP cavity. The rise time of the sensor was less than 4 μs under a pressure up to 8 kPa. In the work by Parkes et al. published in 2007 [11], diaphragms made by different materials were fabricated as the sensing element of a pressure sensor and the results were compared. They used the silicon dioxide and the silicon nitride as the materials of the diaphragm. According to their paper, the sensors made by both of the diaphragms can achieve a rise time of less than 3 μs with a range from 0.1 MPa to 1 MPa. Chavko et al. measured the shock wave in a rat brain by using a fiber optic pressure sensor made by FISO Technologies (Quebec, Canada) [12]. The results indicated that the sensor has a rise time of at least 0.4 ms from 0 kPa to 50 kPa.

In order to better understand how blast waves have an impact on the TBI, distributed sensing is needed. The pressure needs to be recorded at different locations simultaneously. The mechanical and electrical coupling between each sensor should be minimized. Meanwhile, the pressure sensors have to possess a fast response, wide dynamic range and compact size. The performance of the sensors mentioned above may be varied from one another due to the instability of the fabrication method. In this paper, we report on a new fiber optic sensor based on FP cavity principle by using an angle polished fiber. Due to the unique microelectromechanical systems (MEMS) manufacturing technique that was used to fabricate the V-grooves and the diaphragm, all the sensors created in one batch share the same performance. The sensor was tested in a static experiment performed in the lab and a shock

#144481 - $15.00 USD Received 22 Mar 2011; revised 25 Apr 2011; accepted 13 May 2011; published 18 May 2011

tube experiment. The results demonstrated that the new sensor showed a fast rise time with compact size and was suitable for evaluating blast waves.

2. Principle and design of the sensor

The detailed design of the sensor has been described in the ref [8]. The sensor comprises two V-grooves with different widths on a silicon chip, a silicon nitride diaphragm released on the surface of the wider V-groove and a 45° angle polished single mode fiber, which is shown in Fig. 1.

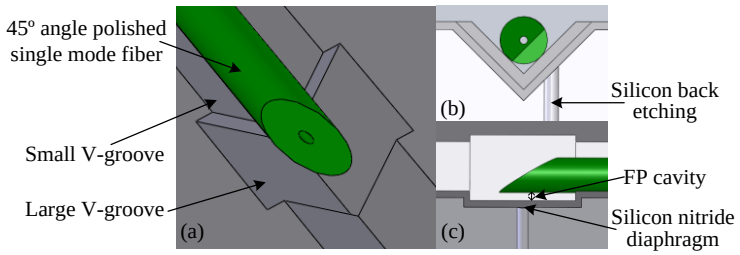

Fig. 1. Schematic diagram of the sensor's design. (a) The sensor comprises two different V-grooves, a silicon nitride diaphragm and an angle polished fiber; (b) Horizontal section view of the hole fabricated by back etching away the silicon substrate; (c) The FP interferometer is formed by the side wall of the angle polished fiber and the silicon nitride diaphragm was released by the back etching.

A silicon substrate was used to fabricate V-grooves. Two V-grooves with different widths were fabricated by anisotropic wet etching. The width difference between two V-grooves determined the FP cavity length. On the surface of the large V-groove, a silicon nitride diaphragm was released by etching away the back side of the silicon substrate. The incident light is guided by the angle polished fiber and reflected on the air-fiber interface and the air-diaphragm interface. Thus, an interference pattern was formed. The excellent alignment between the fiber and the diaphragm provided by the V-grooves promised that the light can be excited on the diaphragm precisely. After the fiber was put in the V-groove and was aligned properly, the fiber was fixed within the V-groove with epoxy. The hole on the back side of the substrate was also sealed with epoxy. Hence, the deformation of the diaphragm was only sensitive to the ambient pressure change. The pressure change can be demodulated from the interference pattern.

By taking advantage of the MEMS technique, the FP cavity length can be precisely controlled by determining the difference of the V-grooves widths. In addition, the sensor's sensitivity and the resonant frequency can also be tailored by precisely controlling the thickness of the silicon nitride diaphragm. For a certain material, the sensitivity and the resonant frequency of a clamped circular diaphragm are related to the diameter and the thickness of the diaphragm. Thus, the sensor has potential to have a variety of properties that can be used for different applications with differing performance requirements. Repeated patterns can be fabricated on the same silicon substrate due to the MEMS technique. This makes such design extremely suitable for sensor arrays and sensor network applications.

3. Sensor fabrication

As described above, the sensor includes two components: the silicon substrate and the angle polished fiber. The fabrication procedure is published in the previous literature [8]. The procedure is repeated here briefly. As shown in Fig. 2, two V-grooves with different widths were fabricated by being etched in potassium hydroxide on a silicon wafer. A thin silicon nitride layer was deposited on the surface of the wafer. In order to release the diaphragm, holes with different diameters were etched from the back side of the wafer. After the silicon substrate was prepared, the angle polished fiber was placed in the V-groove and was aligned

#144481 - $15.00 USD Received 22 Mar 2011; revised 25 Apr 2011; accepted 13 May 2011; published 18 May 2011

to a silicon nitride diaphragm with a specific diameter. The fiber was fixed to the silicon substrate by epoxy. The back side holes were also sealed with epoxy.

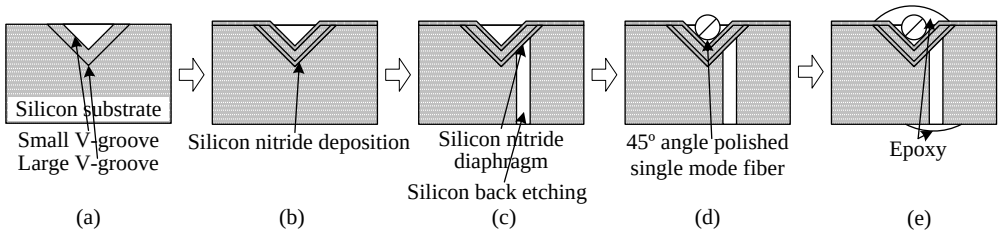

Fig. 2. The schematic diagram of the sensor fabrication procedure. (a) Two V-grooves with different widths were fabricated by anisotropic wet etching on a (100) silicon substrate; (b) A thin film of the silicon nitride was deposited on the surface; (c) A silicon nitride diaphragm was released on the side wall of the large V-groove by etching away the silicon from the backside of the silicon substrate; (d) A 45° angle polished single mode fiber was placed and fixed in the small V-groove; (e) The angle polished fiber and the back holes were sealed with epoxy.

4. Experiments

4.1 Sensor verification

In order to verify the sensor performance and obtain the sensitivity and the hysteresis information from the sensor, a static test was performed. Figure 3 shows the static experimental setup. The optical pressure sensor was placed in a chamber side by side with a commercial pressure sensor (PX303-030G5V, Omega) which was used as a reference sensor. An electro-pneumatic valve (IP413-020, Omega) was used to control the pressure in the chamber. A component test system (CTS) (Si720, Micron Optics) was introduced to detect the reflection interference pattern from the optical pressure sensor. The reflection light and the input light were distinguished by a circulator. The data from CTS and the pressure signal from the reference sensor were recorded by a computer. The fringe of the reflection interference waveform was sensitive to the deformation of the silicon nitride diaphragm. By recording the shift of the wavelength corresponding to the minimum intensity in the interference waveform, the pressure change in the chamber can be determined. The pressure in the chamber was first increased from 0 to 12 psi and then subsequently decreased.

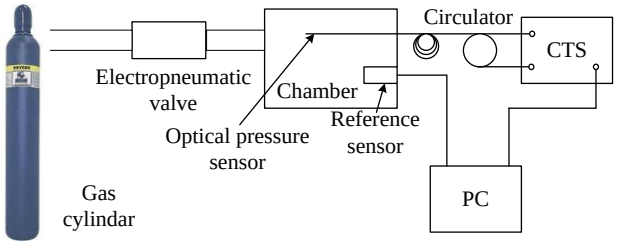

Fig. 3. Schematic diagram of the static experiment setup.

4.2 Test in a shock tube

The purpose of the shock tube test was to characterize the sensor's response to the rapidly changing pressure signal. Because of its low scanning rate (5 Hz), the CTS was not fast enough to follow the rapidly changing pressure signal, which usually rises within milliseconds. The intensity based interrogation system was used. The interference waveform shift can be demodulated from the intensity change of a fixed wavelength laser. The reflection light intensity can be described as $I = I_0[1 + V\cos(\varphi-\varphi_0)]$, where I_0 is the incident light intensity, V is the visibility of the interferometer, $\varphi_0$is a phase constant, φ is the optical phase which is $\varphi = 4\pi nl/\lambda$, where n is the refractive index of the interferometer and l is the cavity

#144481 - $15.00 USD Received 22 Mar 2011; revised 25 Apr 2011; accepted 13 May 2011; published 18 May 2011

length [10]. Therefore, the change of the cavity length corresponding to the pressure change will cause the reflection light intensity change. The light intensity can be interrogated by using a photodetector. The sampling rate of the photodetector can be chosen fast enough to accurately quantify the rapidly changing pressure signal.

The shock tube test was performed at Natick Soldier Research, Development, and Engineering Center (NSRDEC) in Natick, MA. Figure 4 illustrates the schematic diagram of the experiment setup. The shock tube was divided into two chambers with a thin aluminum membrane. One of the chambers was connected to an air compressor. When the pressure in the chamber exceeded the threshold that the membrane could bear, the membrane would suddenly rupture. The high pressure air would rush into the other chamber. At the end of the shock tube, the optical pressure sensor was mounted side by side with a commercial piezoelectric sensor (102A06/ #28592, PCB Piezotronics) as a reference. A tunable laser (TLB-6600, New Focus) which can be fixed at a specific wavelength within the range from 1520 nm to 1570 nm was used to excite the laser into the optical pressure sensor. A variable gain photodetector (PDA10CS, Thorlabs) was introduced to collect the reflection light intensity from the sensor. Both signals from the optical pressure sensor and the electrical reference sensor were collected and stored in a PC through a data acquisition card (DAC) (PCI-6132, National Instruments).

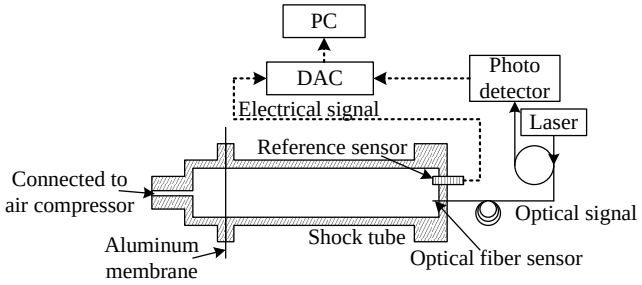

Fig. 4. Schematic diagram of the shock tube experiment.

5. Results and discussions

5.1Fabrication

Figure 5(a) shows a photograph of a typical optical pressure sensor substrate that was ready to be packaged. Multiple V-grooves were fabricated on a single chip. The sensor substrate can be packaged as a single sensor or a sensor array according to different applications. Figure 5(b) illustrates a magnified photograph of the diaphragms that were released on a V-groove. Figure 5(c) shows the magnified photograph of the same diaphragms. The light was illuminated from the back side of the chip. The brighter circles are diaphragms. There were six diaphragms with different diameters fabricated simultaneously. Because of the over etching near the middle of the groove, the diaphragms were not perfect circles. During packaging of the sensor, the 45° angle polished fiber could be aligned to any one of these diaphragms according to different sensitivity requirements. In this paper, a diaphragm with diameter of approximately 80 μm was chosen and the following test results were obtained by using the same diaphragm diameter. The angle polished fiber was placed and fixed with an epoxy. The back side of the sensor was sealed with another piece of silicon chip by epoxy. The packaged sensor with the angle polished fiber is shown in Fig. 5(d).

#144481 - $15.00 USD Received 22 Mar 2011; revised 25 Apr 2011; accepted 13 May 2011; published 18 May 2011

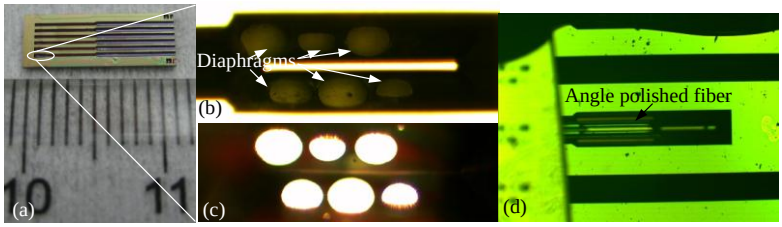

Fig. 5. (a) A photograph of a typical optical pressure sensor substrate which was ready for packaging; (b) Magnified photograph of V-groove with diaphragms of six different diameters; (c) Magnified photograph of diaphragms with transmit light source; (d) A packaged optical pressure sensor with an angle polished fiber in the V-groove. The diameter of the diaphragm was chosen at 80 μm.

5.2 Sensor verification

Figure 6 shows the reflection interference waveform observed on the CTS. The interference waveform showed a redshift when the pressure increased because the length of the FP cavity was increased. The free spectral range (FSR) can be read from the figure as 26.5 nm. The length of the FP cavity can be calculated by FSR = $\lambda_0^2/(2nl\cos\theta)$, where n is the refractive index of the material in the FP cavity; θ is the refractive angle; λ_0 is the central wavelength of the nearest reflection peak; l is the FP cavity length. In this particular case, $n = 1$, $\theta = 0°$ and $\lambda_0 = 1523.5$ nm. Hence, the calculated FP cavity length was 43.8 μm. The desired FP cavity length after fabrication was 44.1 μm according to the designed V-groove width difference. The tiny difference between the calculated value from FSR and the designed value proved that the FP cavity length can be controlled precisely by using MEMS technique. The previous literature [8] demonstrated that the sensor exhibits high linearity with a 0.9999 correlation coefficient and the sensitivity of the sensor is 3.1 nm/kPa

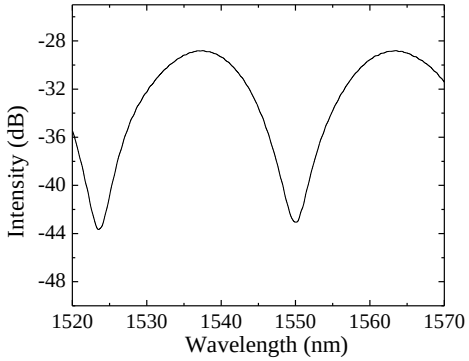

Fig. 6. The reflection interference waveform observed on the CTS. The free spectral range (FSR) was measured as 26.5 nm.

5.3 Shock tube test

In the shock tube test, the optical pressure sensor was mounted on the end plate of the shock tube, positioned side by side with the reference sensor. The photodetector was set to have a 20 dB gain. The DAC's sampling rate was set at 2.5 MHz which is the maximum sampling rate for this kind of DAC. The duration of the sampling data time was set to 0.1 s.

The test results are shown in Fig. 7. Because the acoustic wave bounced back and forth in the shock tube, there were several peaks shown in the whole signal set. Figure 7(a) shows the first cycle of the signal. The pressure was increased from 0 kPa to approximately 140 kPa. The signals from the optical pressure sensor and the reference sensor were similar to each other including the oscillation and the decay time. The oscillation both decayed in a similar time period. Figure 7(b) shows the time zoomed-in data of the rise portion of the signal in Fig.

#144481 - $15.00 USD Received 22 Mar 2011; revised 25 Apr 2011; accepted 13 May 2011; published 18 May 2011

7(a). In the figure, the optical pressure sensor showed a rise time of 2 μs. The time lag between the measurements from the reference sensor and the optical pressure sensor is caused because that the two sensors were not mounted in the exactly the same plane. The shock wave arrived at the optical pressure sensor first and then hit the reference sensor second.

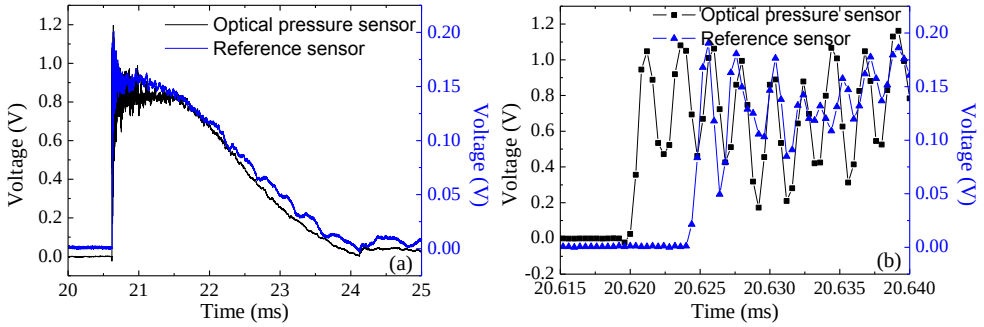

Fig. 7. The experiment results of shock tube test. (a) The first cycle of the blast event; (b) Zoomed-in picture emphasizing on the rise portion of the signal.

However, in Fig. 7(a) from 22 to 25 ms, the amplitude of oscillations that the reference sensor measured was larger than the one that the optical pressure sensor measured. It is likely due to the mounting methods applied to both sensors. The reference sensor was screwed in the end plate whereas the optical pressure sensor was attached to the end plate by an adhesive tape. The double sided tape between the optical pressure sensor and the end plate acted as a cushion that can absorb the energy. Therefore, small changes in the decay portion of the shock wave were likely dampened by the double sided tape.

On the other hand, in the initial portion of the signal, a high frequency oscillation could be observed, which can be seen from Fig. 7(b) and Fig. 8. The same oscillation with the same frequency could be observed repeatedly based on performing another round of tests. It could be caused by the vibration of the end plate after being hit by the shock wave. However, in Fig. 8, the amplitude of oscillations from the optical pressure sensor was larger than that from the reference sensor. The cantilever structure that was formed by the sealed point and the optical fiber when the angle polished fiber was placed inside the V-groove and was sealed with the epoxy could contribute to the larger oscillation. When the shock wave hit on the optical pressure sensor, the optical fiber would vibrate. As a result, the amplitude of the oscillations from the optical pressure sensor was larger.

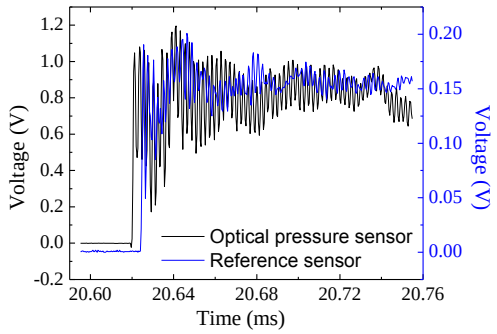

Fig. 8. The initial portion of the signal in Fig. 7(a). The oscillations from the optical pressure sensor were larger than that from the reference pressure sensor due to the cantilever structure.

#144481 - $15.00 USD Received 22 Mar 2011; revised 25 Apr 2011; accepted 13 May 2011; published 18 May 2011

6. Conclusions

This paper presents a fiber optic pressure sensor which can be used for blast event evaluation. The compact size of the sensor will allow for multiple sensors to be distributed over an area to provide a better spatial resolution, helping to understand the dynamics of blast and the interaction between a helmet and the pressure wave. The fabrication of the sensor takes advantages of the MEMS technique so that the high repeatability of the sensor makes it a perfect candidate for sensor array applications. The FP cavity length and mechanical properties of the diaphragm can be adjusted very precisely, therefore the new sensor performance can be tailored for blast wave evaluation monitoring and other applications.

In the static test conducted, the sensor showed good linearity and low hysteresis. Likewise, the shock tube test proved that the sensor had response time fast enough to capture the rapidly changing pressure signal of a blast wave. The test results showed that the sensor featured a rise time of less than 2 μs from 0 kPa to approximately 140 kPa.

Acknowledgments

The authors are grateful for the collaboration with Natick Soldier Research, Development, and Engineering Center for sharing the shock tube and the reference pressure sensors. The authors also appreciate the Army Research Laboratory for sponsoring this work (Nanomanufacturing of Multifunctional Sensors Ref. Award Number: W911NF-07-2-0081).

#144481 - $15.00 USD Received 22 Mar 2011; revised 25 Apr 2011; accepted 13 May 2011; published 18 May 2011